

อิทธิพลของปอช โขลานต่อการแตกร้าวเนื่องจากการหดตัวของแบบพลาสติกของคอนกรีต



ไอริน โอลิเวีย อุโบ

วิทยานิพนธ์นี้เป็นส่วนหนึ่งของการศึกษาตามหลักสูตรปริญญาวิศวกรรมศาสตรมหาบัณฑิต

สาขาวิชาวิศวกรรมโยธา ภาควิชาวิศวกรรมโยธา

คณะวิศวกรรมศาสตร์ จุฬาลงกรณ์มหาวิทยาลัย

ปีการศึกษา 2549

ลิขสิทธิ์ของจุฬาลงกรณ์มหาวิทยาลัย

**INFLUENCE OF POZZOLAN ON THE
PLASTIC SHRINKAGE CRACKING OF CONCRETE**

Miss Irene Olivia Ubay

**A Thesis Submitted in Partial Fulfillment of the Requirements
for the Degree of Master of Engineering Program in Civil Engineering**

Department of Civil Engineering

Faculty of Engineering

Chulalongkorn University

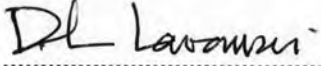
Academic Year 2006

Copyright of Chulalongkorn University

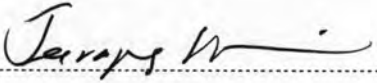
491734


Thesis Title INFLUENCE OF POZZOLAN ON THE PLASTIC
SHRINKAGE CRACKING OF CONCRETE
By Ms. Irene Olivia Ubay
Field of Study Civil Engineering
Thesis Advisor Associate Professor Boonchai Stitmannathum, D.Eng.
Thesis Co-advisor Professor Toyoharu Nawa, Ph.D.

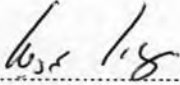
Accepted by the Faculty of Engineering, Chulalongkorn University in Partial
Fulfillment of the Requirements for the Master's Degree

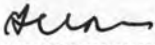
..... Dean of the Faculty of Engineering
(Professor Direk Lavansiri, Ph.D.)


THESIS COMMITTEE

..... Chairman
(Associate Professor Teerapong Senjuntichai, Ph.D.)

..... Thesis Advisor
(Associate Professor Boonchai Stitmannathum, D.Eng.)

..... Member
(Associate Professor Phoonsak Pheinsusom, D.Eng.)

..... Member
(Associate Professor Chai Jaturapitakkul, Ph.D.)

..... Member
(Assistant Professor Chatpan Chintanapakdee, Ph.D.)

Irene Olivia Ubay: อิทธิพลของปอซโซลานต่อการแตกร้าวเนื่องจากการหดตัวของแบบพลาสติกของคอนกรีต (INFLUENCE OF POZZOLAN ON THE PLASTIC SHRINKAGE CRACKING OF CONCRETE) อาจารย์ที่ปรึกษา: รศ.ดร.บุญไชย สถิตมั่นในธรรม, 160 pp.

โดยปกติคอนกรีตสดจะมีรอยแตกร้าวจากการหดตัวของแบบพลาสติกเกิดขึ้นหากอัตราการระเหยของน้ำตรงผิวคอนกรีตมีค่าสูงกว่าอัตราการซึมของคอนกรีตสด รอยแตกร้าวจากการหดตัวของแบบพลาสติกมักเกิดกับโครงสร้างคอนกรีตประเภทแผ่นพื้น ผิวทาง และคอนกรีตซึ่งมีอัตราส่วนของพื้นผิวต่อปริมาตรสูง โดยเป็นที่ยอมรับว่ารอยแตกร้าวนั้นอาจมีความลึกผ่านลงมาตลอดทั้งหน้าตัด นั่นคือหากรอยแตกร้าวมีขนาดใหญ่และกว้างพอจะทำให้สารเคมีต่างๆแทรกซึมเข้าไปทำลายคอนกรีตได้ การใช้ปอซโซลานในงานอุตสาหกรรมคอนกรีตนั้นมีแนวโน้มสูงขึ้นทั้งนี้เป็นเพราะปอซโซลานสามารถปรับปรุงคุณสมบัติด้านต่างๆของคอนกรีตให้ดีขึ้นได้ จึงมีความเป็นไปได้ที่การใช้ปอซโซลานจะสามารถควบคุมการแตกร้าวจากการหดตัวของแบบพลาสติกดังกล่าว อันนำไปสู่การศึกษาในงานวิจัยฉบับนี้ โดยปอซโซลานที่นำมาใช้ในงานวิจัย คือ ถ้ำลอยและซิลิกาฟูม มีสัดส่วนการแทนที่ซีเมนต์ด้วยถ้ำลอยเป็นร้อยละ 0 ถึง 50 โดยน้ำหนักของวัสดุประสาน และสัดส่วนการแทนที่ด้วยซิลิกาฟูมเป็นร้อยละ 0.3 และ 5 โดยน้ำหนักของวัสดุประสาน และผสมโดยใช้สัดส่วนน้ำต่อวัสดุประสานเป็น 0.3 0.4 และ 0.5 การเตรียมและทดสอบตัวอย่างเป็นไปตามมาตรฐาน ASTM C1579-06 โดยในการทดสอบจะทำการถ่ายภาพรอยแตกร้าวบนตัวอย่างและนำภาพที่ได้มาทำการวิเคราะห์เพื่อคำนวณหาการแตกร้าวในลักษณะของพื้นที่รอยแตกร้าว ความกว้างรอยแตกร้าวสูงสุด และความกว้างรอยแตกร้าวเฉลี่ย อีกทั้งยังได้ทำการศึกษาเพื่อเปรียบเทียบผลของการบ่มคอนกรีตต่อพฤติกรรมของรอยแตกร้าวในคอนกรีตที่อายุ 28 วัน ระหว่างการบ่มขึ้นด้วยการใช้กระสอบเปียกคลุมตัวอย่างกับการบ่มแห้งในอากาศภายในห้องทดสอบ จากผลการวิจัยพบว่าเมื่อใช้ถ้ำลอยทดแทนซีเมนต์ในปริมาณสูงขึ้น พื้นที่รอยแตกร้าวจะลดลง ในขณะที่ความกว้างรอยแตกร้าวสูงสุดและความกว้างรอยแตกร้าวเฉลี่ยจะมีค่ามากขึ้น ในกรณีที่ใช้ซิลิกาฟูมทดแทนซีเมนต์พบว่าพื้นที่รอยแตกร้าว ความกว้างรอยแตกร้าวสูงสุดและความกว้างรอยแตกร้าวเฉลี่ยจะมีค่าลดลงเมื่อแทนที่ซีเมนต์ด้วยซิลิกาฟูมในสัดส่วนที่สูงขึ้น อีกทั้งพบว่า การใช้ถ้ำลอยและซิลิกาฟูมในคอนกรีตที่ได้รับการบ่มขึ้นนั้นจะมีอิทธิพลต่อการแตกร้าวที่ทำการวิเคราะห์ได้มากกว่าคอนกรีตที่ถูกบ่มแห้ง

ภาควิชา วิศวกรรมโยธา

สาขาวิชา วิศวกรรมโยธา

ปีการศึกษา 2549

ลายมือชื่อนิติศ.....

ลายมือชื่ออาจารย์ที่ปรึกษา.....

4870643921: MAJOR CIVIL ENGINEERING

KEY WORD: PLASTIC SHRINKAGE CRACKS / POZZOLAN / FLY ASH / SILICA FUME / IMAGE ANALYSIS

IRENE OLIVIA UBAY: THESIS TITLE: INFLUENCE OF POZZOLAN ON THE PLASTIC SHRINKAGE CRACKING OF CONCRETE. THESIS ADVISOR: ASSOC. PROF. BOONCHAI STITMANNAITHUM, D.Eng, 160 pp.

Concrete at its fresh state allows for the occurrence of plastic shrinkage cracks due to the excessive and rapid evaporation rate of water and the inability or lack of bleed water to replace the evaporating water. Plastic shrinkage cracks can occur in concrete slabs, pavements, and flatworks and has been known on occasion to penetrate the whole depth of a section. Unless such cracks are small and narrow, they could permit penetration of deleterious substances and weaken the structure if not controlled. Since the use of pozzolan in the concrete industry has been increasing due to its ability to improve concrete properties, then it would be possible that such materials could provide a means to control plastic shrinkage cracking in concrete. Pozzolan used as cement replacement were fly ash and pelletized silica fume. Fly ash contents of 0 to 50% and silica fume contents of 0, 3, and 5% were mixed with water/binder ratios of 0.30, 0.40, and 0.50. Specimens were prepared and tested in accordance with ASTM C 1579-06. Images of the specimens studied were taken and processed for crack quantification in terms of crack area, maximum crack width, and average crack width with the use of Image Analysis technique. The behavior of the cracks was also observed after 28 days of exposure to different curing conditions: moist curing by wet burlap and exposure to air curing conditions. Results show that with as the amount of fly ash as cement replacement was used, crack area decreased. However, maximum crack width and average crack width increased as fly ash content increased. For silica fume concrete, crack area, maximum crack width, and average crack width decreased as the amount of silica fume increased. Both fly ash and silica fume concrete specimens had greater percent change in crack quantification values when exposed to moist cured conditions.

Department Civil Engineering
Field of study Civil Engineering
Academic year 2006

Student's signature.....

Advisor's signature.....

ACKNOWLEDGEMENTS

My sincerest thanks to my adviser, Assoc. Prof. Dr. Boonchai Stitmannathum, whose patience and continuous assistance throughout the duration of my research made me more driven into accomplishing my goals. Also, thanks to my co-adviser, Prof. Dr. Toyoharu Nawa, who always found time to answer questions and give inspiring thoughts.

I am grateful to my thesis committee members, Assoc. Prof. Dr. Teerapong Senjuntichai, Assoc. Prof. Dr. Phoonsak Pheinsusom, Assoc. Prof. Dr. Chai Jaturapitakkul and Assistant Prof. Dr. Chatpan Chintanapakdee, for their kindness to spend their time to review my work and provide valuable comments and suggestions for improvement.

Thank you to AUN / SEED-Net and JICA for granting me this scholarship and for their financial support for this research. Much appreciation goes to the staff, technicians, and students of the Civil Engineering Department of Chulalongkorn University for their assistance. Much thanks to Lerwate Paksoontorn and Wanich Rattanasinchaiboon for their help in making this research more bearable.

To all my friends under the AUN/SEED-Net scholarship program to whom I consider as my family, thank you for your friendship and support. This experience was truly an unforgettable one because of all of you. I would also like to thank Engr. Ronaldo Gallardo and the Engineering Department of De La Salle University-Manila for all of their support. Special thanks to Mr. Alitking Anongphouth for his continuous encouragement.

I dedicate this thesis to my family who never doubted that I would be able to overcome the challenges that I faced. It is because of their prayers and deep faith that led me towards success. To my parents, Engrs. Renato and Olivia Ubay, thank you for believing in me and for letting me follow your footsteps.

Thank you, God, for this blessing in my life. I am truly grateful.

CONTENTS

	Page
Abstract in Thai	iv
Abstract in English	v
Acknowledgements	vi
Contents	vii
List of Tables	x
List of Figures	xii
CHAPTER I INTRODUCTION	1
1.1 Introduction	1
1.2 Objectives of the Research	2
1.3 Scope of the Research	3
1.4 Significance of the Research	3
CHAPTER II LITERATURE REVIEW	5
2.1 Plastic Shrinkage Cracking of Concrete	5
2.2 Factors Affecting Plastic Shrinkage Cracking	7
2.2 Use of Pozzolan in Concrete	10
2.2.1 Effect of Fly Ash on Plastic Shrinkage Cracking of Concrete	11
2.2.2 Effect of Silica Fume on Plastic Shrinkage Cracking of Concrete	17
CHAPTER III RESEARCH METHODOLOGY	21
3.1 Testing Equipment	21
3.1.1 Specimen Molds	21
3.1.2 Test Chamber	22
3.1.3 Image Analysis Technique	25
3.2 Testing Procedure	29
3.2.1 Test Preparations	29
3.2.1.1 Calibrations	29
3.2.1.1.1 Test Chamber Calibration	29
3.2.1.1.2 Digital Camera Calibration	30
3.2.1.2 Materials and Mix Design	34

	Page
3.2.1.3 Setting Time Tests.....	37
3.2.2 Plastic Shrinkage Cracking Test.....	38
3.2.3 Image Analysis Processing.....	40
3.2.4 Curing Procedure.....	44
3.3 Quantification of Plastic Shrinkage Cracks.....	45
CHAPTER IV RESULTS, ANALYSES, AND DISCUSSIONS.....	48
4.1 Effect of Fly Ash on Plastic Shrinkage Cracking of Concrete.....	48
4.1.1 Properties.....	48
4.1.2 Effect on Average Crack Width.....	51
4.1.3 Effect on Maximum Crack Width.....	59
4.1.4 Effect on Crack Area.....	60
4.1.5 Effect of Curing on Fly Ash Concrete.....	63
4.1.6 Cracking Reduction Ratio of Fly Ash Concrete.....	78
4.1.7 Summary of Results of Fly Ash Concrete.....	80
4.2 Effect of Silica Fume on Plastic Shrinkage Cracking of Concrete.....	83
4.2.1 Properties.....	83
4.2.2 Effect on Average Crack Width.....	84
4.2.3 Effect on Maximum Crack Width.....	87
4.2.4 Effect on Crack Area.....	89
4.2.5 Effect of Curing on Silica Fume Concrete.....	89
4.2.6 Cracking Reduction Ratio of Silica Fume Concrete.....	96
4.2.7 Summary of Results of Silica Fume Concrete.....	97
CHAPTER V CONCLUSIONS AND RECOMMENDATIONS.....	98
5.1 Conclusions.....	98
5.2 Recommendations.....	100
REFERENCES.....	102
APPENDICES.....	105
Index.....	106

	Page
Appendix A Evaporation Rate.....	108
Appendix B Bleeding Rate.....	124
Appendix C Crack Width Measurements.....	126
Appendix D Data Summary.....	143
Appendix E Image Processing Example.....	152
Appendix F Sample Calculation for 40-10FA.....	158
BIOGRAPHY.....	160

LIST OF TABLES

	Page
Table 2.1	Maximum plastic shrinkage strain in plain and blended cement concretes, exposed to a wind velocity of 12 km/h, temperature of 45°C and relative humidity (RH) of 35%..... 19
Table 3.1	List of HyperCube transformation equations..... 32
Table 3.2	Material properties..... 35
Table 3.3	Material chemical composition..... 35
Table 3.4	Primary mix design..... 37
Table 4.1	Properties of fly ash concrete..... 49
Table 4.2	Time of appearance of first crack in fly ash concrete specimens..... 50
Table 4.3	Evaporation rate and environmental conditions during testing of fly ash specimens..... 50
Table 4.4	Statistical parameters of fly ash concrete crack widths..... 51
Table 4.5	Tolerable crack widths for different exposure conditions (ACI 224R)..... 52
Table 4.6	Ninety percentile crack width values of fly ash concrete specimens..... 60
Table 4.7	Number of crack width measurements of fly ash concrete specimens for curing..... 63
Table 4.8	Standard deviation values of cured fly ash concrete specimens..... 70
Table 4.9	Ninety percentile crack width values of chosen fly ash concrete Specimens after curing..... 74
Table 4.10	Mean crack widths of chosen fly ash concrete specimens after curing..... 74
Table 4.11	Physical properties of silica fume concrete..... 83
Table 4.12	Time of appearance of first crack in silica fume concrete specimens..... 84
Table 4.13	Statistical parameters of silica fume concrete crack widths..... 85
Table 4.14	Ninety percentile crack width values of silica fume concrete specimens..... 88
Table 4.15	Number of crack width measurements of silica fume concrete specimens for curing..... 90

Table 4.16	Standard deviation values of cured silica fume concrete specimens.....	92
Table 4.17	Ninety percentile crack width values of chosen silica fume concrete specimens after curing.....	95
Table 4.18	Mean crack width values of chosen silica fume concrete specimens after curing.....	95

LIST OF FIGURES

	Page
Figure 2.1	Cores drilled through cracks through a test slab..... 7
Figure 2.2	Effect of water-cement ratio on time to initiation of cracks..... 9
Figure 2.3	Effect of cement content on total crack area..... 10
Figure 2.4	Effect of (a) water-cement ratio, (b) fly ash content..... 12
	(c) fly ash type on water loss..... 13
Figure 2.5	Effect of fly ash content on total crack area..... 13
Figure 2.6	Effect of fly ash type and content on plastic shrinkage cracking..... 14
Figure 2.7	Effect of fly ash on crack width..... 15
Figure 2.8	Effect of fly ash on crack length..... 15
Figure 2.9	Effect of fly ash on crack area..... 15
Figure 2.10	Total cracking area of mortar mixtures with water-cement ratio of 0.40..... 16
Figure 2.11	Total cracking area of mortar mixtures with water-cement ratio of 0.34..... 16
Figure 2.12	Crack pattern of selected mortar mixtures made with Federal Highway Association (FHWA) Class F fly ash and water-cement ratio of 0.40..... 17
Figure 2.13	Plastic shrinkage of concretes with 5, 10, and 15% silica fume when exposed to 50% relative humidity at 20°C..... 18
Figure 3.1	Specimen molds as specified in ASTM C 1579-06..... 21
Figure 3.2	Existing specimen molds built from specifications..... 22
Figure 3.3	Schematic setting of chamber to maintain environmental conditions..... 23
Figure 3.4	Schematic setting of fan box to maintain environmental conditions..... 24
Figure 3.5	Existing test chamber..... 25
Figure 3.6	Steel stand for taking pictures..... 29
Figure 3.7	Ten cm grid points..... 32
Figure 3.8	Control points of sample paper grid as shown in HyperCube Warp Function..... 33

Figure 3.9	Original digital image of 5cm grid paper for calibration.....	34
Figure 3.10	Corrected image of 5cm grid paper using Cubic-10 term equation of the Warp function in HyperCube.....	34
Figure 3.11	Gradation curve for coarse aggregate.....	36
Figure 3.12	Gradation curve for fine aggregate.....	36
Figure 3.13	Example of control points in text file.....	40
Figure 3.14	Control points of a test specimen as shown in HyperCube Warp Function.....	41
Figure 3.15	Warp function in HyperCube.....	42
Figure 3.16	Original image of a 40-10FA specimen.....	42
Figure 3.17	Corrected image of a 40-10FA specimen using HyperCube.....	43
Figure 3.18	Measurement of crack widths along 5mm grid lines using AutoCAD.....	44
Figure 3.19	Determining crack area from measured crack widths.....	46
Figure 4.1	Histogram plots of crack widths of fly ash concrete specimens with $w/b = 0.30$	52
Figure 4.2	Histogram plots of crack widths of fly ash concrete specimens with $w/b = 0.40$	53
Figure 4.3	Histogram plots of crack widths of fly ash concrete specimens with $w/b = 0.50$	54
Figure 4.4	Normal distribution curves of crack width of fly ash concrete specimens with water/binder ratio = 0.30.....	55
Figure 4.5	Normal distribution curves of crack width of fly ash concrete specimens with water/binder ratio = 0.40.....	56
Figure 4.6	Normal distribution curves of crack width of fly ash concrete specimens with water/binder ratio = 0.50.....	56
Figure 4.7	Effect of fly ash content on average crack width.....	57
Figure 4.8	Effect of fly ash content on maximum crack width.....	59
Figure 4.9	Effect of fly ash content on crack area.....	61
Figure 4.10	General effect of fly ash content on crack area.....	62
Figure 4.11	Normal distribution curve comparison for fly ash concrete specimens under air curing conditions with $w/b = 0.30$	64

Figure 4.12	Normal distribution curve comparison for fly ash concrete specimens under air curing conditions with $w/b = 0.40$	65
Figure 4.13	Normal distribution curve comparison for fly ash concrete specimens under air curing conditions with $w/b = 0.50$	66
Figure 4.14	Normal distribution curve comparison for fly ash concrete specimens under moist curing conditions with $w/b = 0.30$	67
Figure 4.15	Normal distribution curve comparison for fly ash concrete specimens under moist curing conditions with $w/b = 0.40$	68
Figure 4.16	Normal distribution curve comparison for fly ash concrete specimens under moist curing conditions with $w/b = 0.50$	69
Figure 4.17	Effect of fly ash content on percent change in average crack width....	71
Figure 4.18	Effect of fly ash content on percent change in maximum crack width.....	72
Figure 4.19	Effect of fly ash content on percent change in crack area.....	73
Figure 4.20	Effect of duration of air curing on average crack width of fly ash concrete specimens.....	75
Figure 4.21	Effect of duration of air curing on maximum crack width of fly ash concrete specimens.....	76
Figure 4.22	Effect of duration of air curing on crack area of fly ash concrete specimens.....	76
Figure 4.23	Effect of duration of moist curing on average crack width of fly ash concrete specimens.....	77
Figure 4.24	Effect of duration of moist curing on maximum crack width of fly ash concrete specimens.....	77
Figure 4.25	Effect of duration of moist curing on crack area of fly ash concrete specimens.....	78
Figure 4.26	Effect of fly ash content on cracking reduction ratio.....	79
Figure 4.27	Effect of fly ash content on average crack width, maximum crack width, crack area, and cracking reduction ratio with $w/b = 0.30$	81
Figure 4.28	Effect of fly ash content on average crack width, maximum crack width, crack area, and cracking reduction ratio with $w/b = 0.40$	82

Figure 4.29	Effect of fly ash content on average crack width, maximum crack width, crack area, and cracking reduction ratio with $w/b = 0.50$	82
Figure 4.30	Histogram plots of crack widths of silica fume concrete specimens.....	85
Figure 4.31	Normal distribution curve of crack width of silica fume concrete specimens.....	86
Figure 4.32	Effect of silica fume content on average crack width.....	87
Figure 4.33	Effect of silica fume content on maximum crack width.....	88
Figure 4.34	Effect of silica fume content on crack area.....	89
Figure 4.35	Normal distribution curve comparison for silica fume concrete specimens under air curing conditions.....	91
Figure 4.36	Normal distribution curve comparison for silica fume concrete specimens under moist curing conditions.....	92
Figure 4.37	Effect of silica fume content on percent change in average crack width.....	93
Figure 4.38	Effect of silica fume content on percent change in maximum crack width.....	94
Figure 4.39	Effect of silica fume content on percent change in crack area.....	94
Figure 4.40	Effect of silica fume content on cracking reduction ratio.....	96
Figure 4.41	Effect of silica fume content on average crack width, maximum crack width, crack area, and cracking reduction ratio.....	97